

## The steady shear viscosity of filled polymeric liquids described by a linear superposition of two relaxation mechanisms

T. S. Stephens, H. H. Winter and M. Gottlieb

Department of Chemical Engineering, University of Massachusetts, Amherst, Mass. (U.S.A.)

**Abstract:** Filled polymeric liquids often exhibit apparent yielding and shear thinning in steady shear flow. Yielding results from non-hydrodynamic particle–particle interactions, while shear thinning results from the non-Newtonian behavior of the polymer melt. A simple equation, based on the linear superposition of two relaxation mechanisms, is proposed to describe the viscosity of filled polymer melts over a wide range of shear rates and filler volume fraction.

The viscosity is written as the sum of two generalized Newtonian liquid models. The resulting equation can describe a wide range of shear-thinning viscosity curves, and a hierarchy of equations is obtained by simplifying the general case. Some of the parameters in the equation can be related to the properties of the unfilled liquid and the solid volume fraction. One adjustable parameter, a yield stress, is necessary to describe the viscosity at low rates where non-hydrodynamic particle–particle interactions dominate. At high shear rates, where particle–particle interactions are dominated by interparticle hydrodynamics, no adjustable parameters are necessary. A single equation describes both the high and low shear rate regimes. Predictions of the equation closely fit published viscosity data of filled polymer melts.

**Key words:** Steady shear viscosity, suspension, filled polymer melt, yield stress

### Symbols

|                          |  |
|--------------------------|--|
| $n$                      | power-law index                                  |
| $n_1, n_2$               | power-law index of first (second) term           |
| $\dot{\gamma}$           | shear rate                                       |
| $\eta$                   | steady shear viscosity                           |
| $\eta_0$                 | zero-shear rate viscosity                        |
| $\eta_{0,1}, \eta_{0,2}$ | zero-shear rate viscosity of first (second) term |
| $\lambda$                | time constant                                    |
| $\lambda_1, \lambda_2$   | time constant of first (second) term             |
| $\mu_r$                  | relative viscosity of filled Newtonian liquid    |
| $\tau_0$                 | yield stress                                     |
| $\phi$                   | solid volume fraction                            |
| $\phi_m$                 | maximum solid volume fraction                    |

### 1. Introduction

The shear-rate dependence of the steady shear viscosity of particle-filled polymeric liquids has recently been reviewed by Metzner [1] and Kamal and Mutel [2]. What

is lacking is an equation, relating the shear viscosity to the shear rate, which is simple enough to be useful and yet captures the important features of the rheological behavior of filled polymers undergoing steady shear. Previously proposed equations are either very complicated [3, 4] or do not accurately describe the shear-rate dependence of viscosity over a wide range of shear rates and concentrations of filler [5, 6].

A typical steady-shear viscosity curve for a filled polymeric liquid is shown in figure 1, which exhibits a “yielding” region at low rates, a plateau region at intermediate rates, and a power-law region at high rates.

Filled polymeric liquids often exhibit a yield stress in shear flow. However, the existence of a true yield stress has been debated [7] and what appears to be yielding may actually be severe shear thinning of a macroscopic structure in the suspension. Matsumoto et al. [8] have found that, for a suspension of styrene-divinylbenzene copolymer spheres in a polystyrene solution which exhibits an

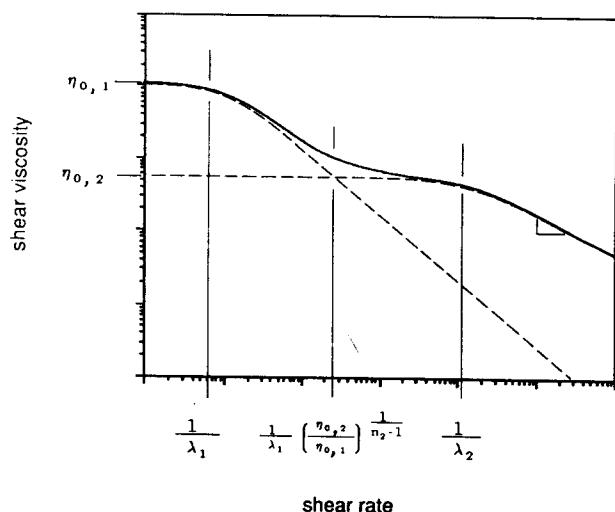


Fig. 1. Typical steady shear viscosity curve for a filled polymer melt (solid curve). Dashed lines show the contribution of each term in eq. (1)

apparent yield stress, a flow region exists at very low shear stress. Matsumoto et al. [9] have shown that a permanent electric charge on the styrene-divinylbenzene copolymer spheres causes the apparent yielding of the suspension to disappear. Suspensions of coal particles in various liquids exhibit apparent viscosities which depend on the polarity of the suspending liquid [10]. Surface treatment of filler particles changes the apparent viscosity suspensions in low-viscosity liquids [11]. These observations suggest that the apparent yield stress originates from particle-particle interactions which are non-hydrodynamic in nature. These non-hydrodynamic interactions depend on electrical and chemical properties of the particles and the particle-fluid interface, such as surface charge, surface potential, or the presence of a surfactant layer.

At higher deformation rates, the non-hydrodynamic forces on the particles are dominated by the stress in the fluid, which is determined by the hydrodynamics in the fluid between the particles. The interparticle hydrodynamics depends on the rheological properties of the fluid and the arrangement of the particles. Experimental observations of the motion of suspended particles have been reviewed by Giesekus [12]. Strings of particles have been observed in suspensions of glass beads in a polyisobutylene solution [13]. Layers of hexagonally packed particles have been observed for concentrated suspensions of monodisperse spheres sheared between parallel plates [14, 15]. The shear-induced particle arrangement is anisotropic and depends on the direction of shearing [16]. Gadala-Maria and Acrivos [17] report that suspensions of polystyrene spheres in silicone oil exhibited a memory

of the direction of shearing when the volume fraction of spheres was greater than 0.3.

Different arrangements of the particles can arise in different types of flow. Thus, the behavior of a suspension in shear flow can be different than in an extensional flow [15]. However, even for shear flow the structure may depend on the specific shear flow geometry: shear flow between parallel plates and shear flow in a cone and plate rotational rheometer can exhibit different values of the steady shear viscosity [18]. A possible explanation for this phenomenon might be that the gradient of the rate of deformation tensor affects the flow induced structure and hence the stress. If this hypothesis is true then the filled liquids are non-simple liquids, since their behavior violates the principle of "local action" (this states that the stress in a fluid element is determined by the deformation history of that fluid element and is independent of the history of neighboring elements). This phenomenon has not been explored much and will be neglected in the rest of the paper by assuming that the shear-rate-dependent viscosity, as measured in one geometry, is predictive for shear flows in other geometries.

Filled polymeric liquids are viscoelastic and exhibit memory and normal stresses in shear flow [19]. This viscoelasticity is not apparent in the shear stress of steady shear flow as will be discussed, however, it would have to be considered in a constitutive equation for the transient mechanical behavior of the filled system.

A sudden viscosity increase at high shear rates ( $10-1000 \text{ s}^{-1}$ ) has been observed for highly concentrated suspensions of micrometer-diameter plastic spheres in low viscosity liquids [14, 20]. This effect does not seem to occur in filled polymer melts, for which the viscosity is observed to monotonically decrease with shear rate.

Highly concentrated suspensions exhibit wall slip in capillaries and in Couette viscometers [21]. Migration of filler particles due to particle concentration gradients has been reported by Leighton and Acrivos [22]. These effects will not be considered here.

## 2. Phenomenological equation

The rheology of filled polymeric liquids depends, in a very complex way, on the structural states of the particles and the fluid. However, there seem to be two limiting flow regimes for which the flow behavior might be expressed in a simplified form. At low deformation rates, the stress is dominated by the non-hydrodynamic interactions of the particles. At higher deformation rates, the stress is dominated by interparticle hydrodynamics which depend on the rheological behavior of the suspending fluid and on the arrangement of the particles. A general constitu-

tive equation would have to describe the particle interaction regime (apparent yielding) at very low deformation rates and non-linear viscoelastic behavior at higher deformation rates. The following will be restricted to a macroscopic phenomenological description of steady shear flow without attempting to derive a general constitutive equation.

A typical steady shear viscosity curve for a filled polymeric liquid is shown in figure 1. We propose that a linear superposition of two components may fit the observed shape of the viscosity curve

$$\eta(\dot{\gamma}) = \eta_I(\dot{\gamma}) + \eta_{II}(\dot{\gamma}) \quad (1)$$

where each component has a constant value at low shear rates and exhibits shear-thinning behavior at high rates. Inherent in this equation is the assumption that the stresses due to non-hydrodynamic and hydrodynamic effects are additive. This assumption seems to be valid at very high or very low shear rates when one of the terms dominates and thus, non-additive contributions are negligible. However, the above equation may be insufficient for structural fluids at shear rates in which the two effects are of comparable magnitude. The range of validity will be explored by comparison with experimental data from the literature.

The shear rate dependence of the two terms of eq. (1) will be very different, because the two terms represent momentum transport by very different mechanisms. For a material with memory, the shear-rate dependence of the steady shear viscosity is determined by the rates of relaxation processes which occur in the material. In filled polymeric liquids, non-hydrodynamic interactions relax very slowly, and give rise to apparent yielding at very low shear rates, whereas hydrodynamic interactions relax quickly, and give rise to shear thinning at high shear rates.

The proposed behavior, eq. (1), may readily be expressed by superposition of two Carreau [23] type power-law models:

$$\eta(\dot{\gamma}) = \eta_{0,1} [1 + (\lambda_1 \dot{\gamma})^2]^{\frac{n_1-1}{2}} + \eta_{0,2} [1 + (\lambda_2 \dot{\gamma})^2]^{\frac{n_2-1}{2}}. \quad (2)$$

Eq. (2) is valid for positive and negative shear rates. Here, for simplicity, the symbol  $\dot{\gamma}$  will denote the magnitude of the rate of deformation tensor

$$\dot{\gamma} = \sqrt{(\dot{\gamma} : \dot{\gamma})/2} \quad (3)$$

which is always non-negative.

Four regions are apparent in the proposed viscosity curve of figure 1: a low shear rate plateau, an apparent yielding region, an intermediate plateau, and a shear thinning region. These four regions are distinct when the following groups of parameters are ordered in magni-

tude:

$$\frac{1}{\lambda_1} < \frac{1}{\lambda_1} \left( \frac{\eta_{0,2}}{\eta_{0,1}} \right)^{\frac{1}{n_2-1}} < \frac{1}{\lambda_2}. \quad (4)$$

The four regions are delimited by the parameters appearing in eq. (2):

$$\text{I) low shear rate plateau, } \dot{\gamma} < \frac{1}{\lambda_1}, \quad (5)$$

$$\text{II) apparent yielding, } \frac{1}{\lambda_1} < \dot{\gamma} < \frac{1}{\lambda_1} \left( \frac{\eta_{0,2}}{\eta_{0,1}} \right)^{\frac{1}{n_2-1}}, \quad (6)$$

$$\text{III) intermediate plateau, } \frac{1}{\lambda_1} \left( \frac{\eta_{0,2}}{\eta_{0,1}} \right)^{\frac{1}{n_2-1}} < \dot{\gamma} < \frac{1}{\lambda_2}, \quad (7)$$

$$\text{IV) shear thinning, } \frac{1}{\lambda_2} < \dot{\gamma}. \quad (8)$$

The first term in eq. (2) contains the non-hydrodynamic effects, which dominate at very low shear rates; describes the apparent yielding and is dependent on the properties of the particles. The second term contains the interparticle hydrodynamic effects, which dominate at high shear rates, and is dependent upon the rheological behavior of the fluid and the particle volume fraction. It is interesting to note that a single equation is able to describe effects of both types.

In the following, several simplifications of eq. (2) will be examined. Some parameters will be eliminated, and others will be related to physical parameters of the system.

### 2.1 Apparent yield stress

A material which possesses a true yield stress has an infinite zero-shear viscosity, and the shear stress approaches a constant as the shear rate approaches zero, making the viscosity at low rates vary inversely with shear rate. At low shear rates, filled polymer melts exhibit a large viscosity which decreases quickly with increasing shear rate. This severe shear thinning of a filled polymer melt at low rates may not be due to a true yield stress, but to a very slow relaxation mechanism. This behavior can be described by choosing very large values for the zero-shear rate viscosity,  $\eta_{0,1}$ , and the first time constant,  $\lambda_1$ . The power-law parameter  $n_1$  may vary from 0 to 1.

If the power-law index  $n_1$  is chosen to be close to zero, then for shear rate region II, given by eq. (6), the shear stress will be almost independent of the shear rate, and the viscosity will be nearly inversely proportional to the shear rate. Eq. (2) then describes the viscosity of a shear-thinning material which exhibits an apparent yield stress, but which possesses a finite zero-shear rate viscosity.

depend in some simple way on the rheological properties of the polymer melt and the volume fraction of the filler. An attempt will be made to predict the values of these parameters.

For a suspension of spherical particles which interact hydrodynamically, the stress is determined by the interparticle kinematics and the rheological properties of the fluid. It is assumed that the particle arrangement is independent of the deformation rate. It seems plausible that the steady shear viscosity of a suspension can be predicted from the rheological properties of the suspending fluid and the particle volume fraction. It has been observed [24] that the stress in a filled polymer melt, as a function of shear rate, is the same as the stress in the pure fluid, as a function of shear rate, evaluated at a shear rate which is higher by a factor depending only on the particle volume fraction. That is, the shear stress in a filled polymer melt may be written as a function of the shear rate and particle volume fraction as

$$\tau(\phi, \dot{\gamma}) = f(\phi) \tau(0, \dot{\gamma}). \quad (19)$$

The shear stress as a function of shear rate is "shifted" to lower shear rates by the presence of filler particles.

The viscosity of a suspension as a function of volume fraction and shear rate is then given by

$$\eta(\phi, \dot{\gamma}) = f(\phi) \eta(0, f(\phi) \cdot \dot{\gamma}). \quad (20)$$

Eq. (20) motivates the choice for the factor  $f(\phi)$  of the relative viscosity of a suspension of spheres in a Newtonian liquid  $\mu_r = f(\phi)$  is defined as the ratio of the viscosity of the suspension to that of the pure fluid. Here, it is assumed that for a suspension in a non-Newtonian fluid, the factor  $f(\phi)$  may be approximated by the relative viscosity. The viscosity of a suspension of spheres in a non-Newtonian liquid, in the absence of non-hydrodynamic particle-particle interactions, may be written

$$\eta(\phi, \dot{\gamma}) = \mu_r(\phi) \eta(0, \mu_r(\phi) \cdot \dot{\gamma}) \quad (21)$$

where  $\mu_r(\phi)$  is the relative viscosity of a suspension of spheres in a Newtonian liquid in the absence of non-hydrodynamic particle-particle interactions.

The relative viscosity of suspensions of rigid spheres in Newtonian liquids in the absence of non-hydrodynamic particle-particle interactions as a function of volume fraction of spheres  $\phi$  is well known [25], and many equations are available to describe this dependence [26]. A simple but accurate equation is that of Graham et al. [27]:

$$\mu_r(\phi) = \left\{ 1 - \phi \left[ 1 + \left( \frac{1 - \phi_m}{\phi_m} \right) \left( 1 - \left( \frac{\phi_m - \phi}{\phi_m} \right)^2 \right)^{1/2} \right] \right\}^{-2.5} \quad (22)$$

where  $\phi_m$  is the maximum solid volume fraction of the filler, which is assumed here to be that of close hexagonal

packing of uniform spheres which equals  $\pi\sqrt{2}/6$ . For  $\phi_m = \pi\sqrt{2}/6$ , eq. (22) becomes

$$\mu_r(\phi) = \{1 - \phi[1 + (0.331\phi - 0.224\phi^2)^{1/2}]\}^{-2.5}. \quad (23)$$

Particle size distributions are not considered here, but may be included by allowing the maximum packing fraction  $\phi_m$  to depend on the particle-size distribution.

The parameter  $\eta_0$  in eq. (12) represents the viscosity of the suspension in region III, given by eq. (14). At these shear rates, non-hydrodynamic particle-particle interactions which give rise to the apparent yield stress are negligible, and the fluid between the particles is being deformed at rates below which shear thinning occurs and may be considered to be a linear viscoelastic fluid. The additivity assumption of eq. (1) implies that non-hydrodynamic effects are accounted for in the first term, and the second term depends only on hydrodynamic effects. If the viscoelasticity of the fluid is negligible, the observed viscosity of the filled fluid will be similar to that of a filled Newtonian fluid. However, since the flow between the particles is unsteady, it is not obvious that viscoelasticity of the fluid can be neglected. It is assumed here that the transient effects of viscoelasticity average out and that the steady shear viscosity of a filled polymeric fluid, in the absence of non-hydrodynamic particle-particle interactions has the same dependence on the volume fraction of solid as a filled Newtonian fluid:

$$\eta_0(\phi) = \mu_r(\phi) \eta_0(0). \quad (24)$$

Once the zero-shear rate viscosity of the unfilled polymer melt  $\eta_0(0)$  is known, the parameter  $\eta_0(\phi)$  is predicted for the filled polymer melt by eq. (24).

The maximum time constant  $\lambda(0)$  of the unfilled polymer melt represents the reciprocal of the shear rate above which the polymer melt shear thins. Eq. (21) predicts the zero-shear rate viscosity and the time constant of the filled fluid to have the same dependence on the volume fraction of solid. The time constant of the filled fluid is then taken to be

$$\lambda(\phi) = \mu_r(\phi) \lambda(0). \quad (25)$$

Eq. (25) predicts the time constant of the filled fluid from the time constant of the unfilled melt.

Eq. (21) also predicts that the viscosity curve for the filled fluid at high shear rates, where non-hydrodynamic forces are negligible, has the same shape as that of the unfilled melt, but is shifted to higher viscosities and to lower shear rates. Gleissle and Baloch [24] have shown that the viscosity curves of filled silicone oils can be superimposed by shifting. Nicodemo and Nicolais [28] used a shifting procedure to superimpose viscosity curves for glass bead-filled polymer solutions, but found that the horizontal shift was different from the vertical shift.

No yield stress appears explicitly in the equation, and it can be used at all stress levels. For a material with a true yield stress, the zero-shear rate viscosity is infinite, and a separate equation is required to describe the rheological behavior at stress levels below the yield stress.

## 2.2 Explicit yield stress

Although the yield stress does not appear explicitly in eq. (2), when the parameter  $n_1$  is close to zero the value of the apparent yield stress can be calculated:

$$\tau_0 = \frac{\eta_{0,1}}{\lambda_1}. \quad (9)$$

Often the low shear rate plateau (region I) is not observed. In this case, the zero-shear rate viscosity  $\eta_{0,1}$  is too large to measure, region II extends to rates too low to measure, and the parameters  $\eta_{0,1}$  and  $\lambda_1$  cannot be determined individually from experimental data. For describing data in the measurable shear rate range, the zero-shear rate limit  $\eta_{0,1}$  and the time constant  $\lambda_1$  are conveniently taken to be infinite.

$$\eta_{0,1} \rightarrow \infty, \quad \lambda_1 \rightarrow \infty. \quad (10)$$

However, the ratio of the zero-shear rate viscosity to the time constant of the first term is taken to be a constant  $\tau_0$  which can be identified as the yield stress, as given by eq. (9). For a true yield stress, the first power-law exponent  $n_1$  is chosen to be zero. Noting that for very large values of  $\lambda_1$ , at measurable shear rates,

$$\lambda_1 \dot{\gamma} \gg 1. \quad (11)$$

Eq. (2) may be rewritten (suppressing unnecessary subscripts):

$$\eta = \tau_0 \dot{\gamma}^{-1} + \eta_0 [1 + (\lambda \dot{\gamma})^2]^{\frac{n-1}{2}}. \quad (12)$$

Eq. (12) describes a viscosity curve as shown in figure 2. Three regions of the viscosity curve are apparent: a yielding region at low rates, a constant viscosity region at intermediate rates, and a shear-thinning region at high rates. The three remaining regions are delimited, in terms of the parameters, by:

$$\text{II) yielding,} \quad \dot{\gamma} < \frac{\tau_0}{\eta_0}, \quad (13)$$

$$\text{III) constant viscosity,} \quad \frac{\tau_0}{\eta_0} < \dot{\gamma} < \frac{1}{\lambda}, \quad (14)$$

$$\text{IV) shear thinning,} \quad \frac{1}{\lambda} < \dot{\gamma}. \quad (15)$$

Eq. (12) contains the yield stress explicitly and can be used only when the magnitude of the stress exceeds the

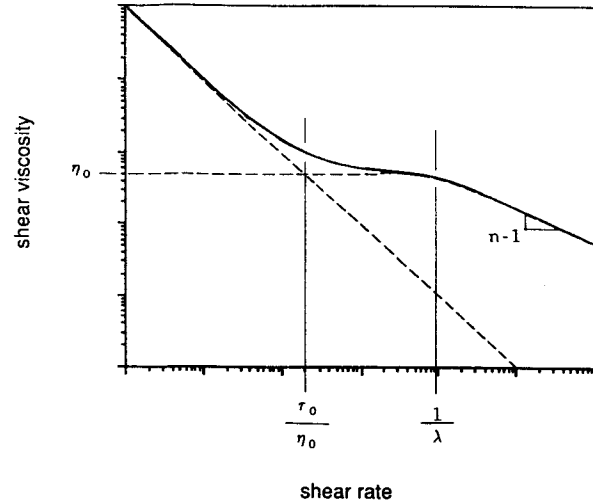


Fig. 2. Viscosity curve showing no low shear rate plateau

yield stress. A second equation is required to describe the deformation at stress magnitudes below the yield stress.

## 2.3 No intermediate plateau

For materials such as very highly filled polymer melts, which possess a large yield stress, and for which the onset of shear thinning occurs at modest shear rates, the constant viscosity region may not exist [19]. For this case, at low to moderate shear rates,

$$\tau_0 \dot{\gamma} \gg \eta_0 [1 + (\lambda \dot{\gamma})^2]^{\frac{n-1}{2}}, \quad (16)$$

and at moderate to high shear rates,

$$(\lambda \dot{\gamma})^2 \gg 1, \quad (17)$$

and eq. (12) simplifies to:

$$\eta = \tau_0 \dot{\gamma}^{-1} + A \dot{\gamma}^{n-1} \quad (18)$$

where  $A = \eta_0 \lambda^{n-1}$  is a lumped parameter. Eq. (18) is identical to the equation of Herschel and Bulkley [5].

## 3. Prediction of the parameters $\eta_0$ , $\lambda$ , and $n$ from the properties of the unfilled melt and the solid volume fraction

The yield stress  $\tau_0$  is assumed to depend on the particle volume fraction and on other properties of the particles which determine the non-hydrodynamic particle-particle interactions. The yield stress is difficult to predict a priori and will remain, in this study, an adjustable parameter. However, the parameters  $\eta_0$ ,  $\lambda$ , and  $n$  are assumed to

depend in some simple way on the rheological properties of the polymer melt and the volume fraction of the filler. An attempt will be made to predict the values of these parameters.

For a suspension of spherical particles which interact hydrodynamically, the stress is determined by the interparticle kinematics and the rheological properties of the fluid. It is assumed that the particle arrangement is independent of the deformation rate. It seems plausible that the steady shear viscosity of a suspension can be predicted from the rheological properties of the suspending fluid and the particle volume fraction. It has been observed [24] that the stress in a filled polymer melt, as a function of shear rate, is the same as the stress in the pure fluid, as a function of shear rate, evaluated at a shear rate which is higher by a factor depending only on the particle volume fraction. That is, the shear stress in a filled polymer melt may be written as a function of the shear rate and particle volume fraction as

$$\tau(\phi, \dot{\gamma}) = f(\phi) \tau(0, \dot{\gamma}). \quad (19)$$

The shear stress as a function of shear rate is "shifted" to lower shear rates by the presence of filler particles.

The viscosity of a suspension as a function of volume fraction and shear rate is then given by

$$\eta(\phi, \dot{\gamma}) = f(\phi) \eta(0, f(\phi) \cdot \dot{\gamma}). \quad (20)$$

Eq. (20) motivates the choice for the factor  $f(\phi)$  of the relative viscosity of a suspension of spheres in a Newtonian liquid  $\mu_r - f(\phi)$  is defined as the ratio of the viscosity of the suspension to that of the pure fluid. Here, it is assumed that for a suspension in a non-Newtonian fluid, the factor  $f(\phi)$  may be approximated by the relative viscosity. The viscosity of a suspension of spheres in a non-Newtonian liquid, in the absence of non-hydrodynamic particle-particle interactions, may be written

$$\eta(\phi, \dot{\gamma}) = \mu_r(\phi) \eta(0, \mu_r(\phi) \cdot \dot{\gamma}) \quad (21)$$

where  $\mu_r(\phi)$  is the relative viscosity of a suspension of spheres in a Newtonian liquid in the absence of non-hydrodynamic particle-particle interactions.

The relative viscosity of suspensions of rigid spheres in Newtonian liquids in the absence of non-hydrodynamic particle-particle interactions as a function of volume fraction of spheres  $\phi$  is well known [25], and many equations are available to describe this dependence [26]. A simple but accurate equation is that of Graham et al. [27]:

$$\mu_r(\phi) = \left\{ 1 - \phi \left[ 1 + \left( \frac{1 - \phi_m}{\phi_m} \right) \left( 1 - \left( \frac{\phi_m - \phi}{\phi_m} \right)^2 \right)^{1/2} \right] \right\}^{-2.5} \quad (22)$$

where  $\phi_m$  is the maximum solid volume fraction of the filler, which is assumed here to be that of close hexagonal

packing of uniform spheres which equals  $\pi\sqrt{2}/6$ . For  $\phi_m = \pi\sqrt{2}/6$ , eq. (22) becomes

$$\mu_r(\phi) = \{1 - \phi [1 + (0.331\phi - 0.224\phi^2)^{1/2}]\}^{-2.5}. \quad (23)$$

Particle size distributions are not considered here, but may be included by allowing the maximum packing fraction  $\phi_m$  to depend on the particle-size distribution.

The parameter  $\eta_0$  in eq. (12) represents the viscosity of the suspension in region III, given by eq. (14). At these shear rates, non-hydrodynamic particle-particle interactions which give rise to the apparent yield stress are negligible, and the fluid between the particles is being deformed at rates below which shear thinning occurs and may be considered to be a linear viscoelastic fluid. The additivity assumption of eq. (1) implies that non-hydrodynamic effects are accounted for in the first term, and the second term depends only on hydrodynamic effects. If the viscoelasticity of the fluid is negligible, the observed viscosity of the filled fluid will be similar to that of a filled Newtonian fluid. However, since the flow between the particles is unsteady, it is not obvious that viscoelasticity of the fluid can be neglected. It is assumed here that the transient effects of viscoelasticity average out and that the steady shear viscosity of a filled polymeric fluid, in the absence of non-hydrodynamic particle-particle interactions has the same dependence on the volume fraction of solid as a filled Newtonian fluid:

$$\eta_0(\phi) = \mu_r(\phi) \eta_0(0). \quad (24)$$

Once the zero-shear rate viscosity of the unfilled polymer melt  $\eta_0(0)$  is known, the parameter  $\eta_0(\phi)$  is predicted for the filled polymer melt by eq. (24).

The maximum time constant  $\lambda(0)$  of the unfilled polymer melt represents the reciprocal of the shear rate above which the polymer melt shear thins. Eq. (21) predicts the zero-shear rate viscosity and the time constant of the filled fluid to have the same dependence on the volume fraction of solid. The time constant of the filled fluid is then taken to be

$$\lambda(\phi) = \mu_r(\phi) \lambda(0). \quad (25)$$

Eq. (25) predicts the time constant of the filled fluid from the time constant of the unfilled melt.

Eq. (21) also predicts that the viscosity curve for the filled fluid at high shear rates, where non-hydrodynamic forces are negligible, has the same shape as that of the unfilled melt, but is shifted to higher viscosities and to lower shear rates. Gleissle and Baloch [24] have shown that the viscosity curves of filled silicone oils can be superimposed by shifting. Nicodemo and Nicolais [28] used a shifting procedure to superimpose viscosity curves for glass bead-filled polymer solutions, but found that the horizontal shift was different from the vertical shift.

If the shape of the viscosity curve of a polymer melt in the shear thinning region (region IV) is maintained with the addition of filler, then the power-law index of the filled melt is the same as that of the unfilled melt. It is assumed here that the power-law index is independent of solid volume fraction. Eq. (12) may be rewritten, using eqs. (24) and (25):

$$\eta(\phi, \dot{\gamma}) = \tau_0 \dot{\gamma}^{-1} + \eta_0 f(\phi) [1 + (\lambda f(\phi) \dot{\gamma})^2]^{\frac{n-1}{2}} \quad (26)$$

where

$$f(\phi) = (1 - \phi [1 + (0.331\phi - 0.224\phi^2)^{1/2}])^{-2.5}. \quad (27)$$

The yield stress  $\tau_0$  is the only remaining adjustable parameter.

#### 4. Application of the proposed equation to filled polymeric liquids

Eq. (26) was used to fit the data of Minagawa and White [19], for four different polymer melts filled with titanium dioxide having an average particle size of  $0.18 \mu\text{m}$  as shown in figures 3–6. The parameters chosen for these fits are listed in table 1. Good agreement between theory and experimental results is obtained for these four different filled melts. It appears that the viscosity parameter  $\eta_0$  and the time constant  $\lambda$  exhibit the same dependence on the solid volume fraction  $\phi$  as the viscosity of a filled Newtonian liquid.

Viscosity data of Gleissle and Baloch [24] for a silicone oil filled with  $50 \mu\text{m}$  diameter coal particles are shown in figure 7 with the viscosity predicted by eq. (26). The parameters chosen for these curves are listed in table 2. The yield stresses for the coal filled silicone oil are much smaller than those of the titanium dioxide suspensions. The hydrodynamic forces on the particles increase with particle size, the non-hydrodynamic forces decrease with particle size, and the yielding behavior is suppressed for suspensions of larger particles.

Suspensions of glass beads with particle diameters of  $40$  to  $80 \mu\text{m}$  in polydimethylsiloxane (General Electric Viscasil 600 000) were prepared, and the steady shear viscosities were measured for a range of shear rates from  $10^{-4}$  to  $10^4 \text{ s}^{-1}$  [29]. A parallel-plate rheometer (Rheometrics RSR) was used for measurements at shear rates from  $10^{-4}$  to  $10^0 \text{ s}^{-1}$ , and a capillary rheometer (Goettfert Rheograph 2001) was used at shear rates from  $10^{-1}$  to  $10^4 \text{ s}^{-1}$ . The viscosities of the unfilled polydimethylsiloxane and of  $50 \text{ vol}\%$  suspensions are shown in figure 8 with the viscosities predicted by eq. (26) using the parameters listed in table 3. A low value of the yield stress was used to fit the curve. The shape of the

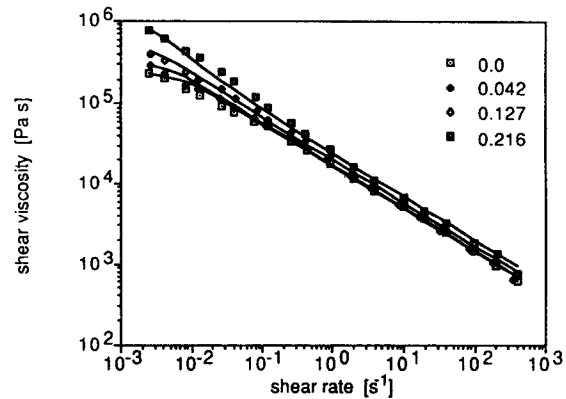


Fig. 3. Steady shear viscosity of  $\text{TiO}_2$ -filled HDPE-0.1 at  $180^\circ\text{C}$ . Data taken from Minagawa and White [19]; solid curve calculated from eq. (11) using the parameters listed in table 1

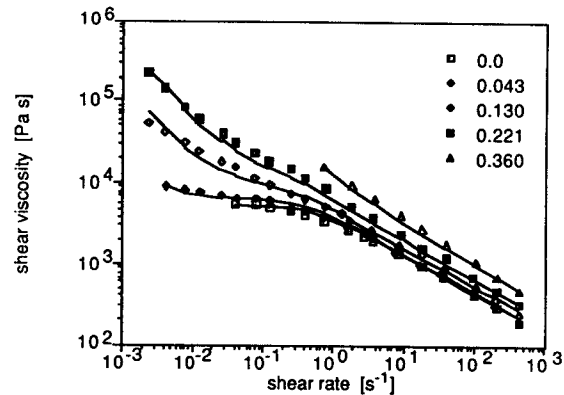


Fig. 4. Steady shear viscosity of  $\text{TiO}_2$ -filled LDPE-5 at  $180^\circ\text{C}$ . Data taken from Minagawa and White [19]; solid curve calculated from eq. (11) using the parameters listed in table 1

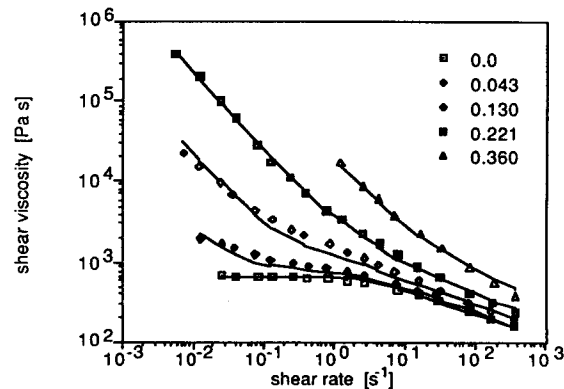


Fig. 5. Steady shear viscosity of  $\text{TiO}_2$ -filled LDPE-23 at  $180^\circ\text{C}$ . Data taken from Minagawa and White [19]; solid curve calculated from eq. (11) using the parameters listed in table 1

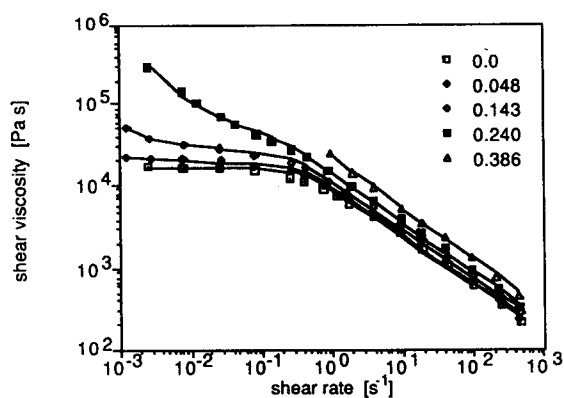


Fig. 6. Steady shear viscosity of  $\text{TiO}_2$ -filled Polystyrene at  $180^\circ\text{C}$ . Data taken from Minagawa and White [19]; solid curve calculated from eq. (11) using the parameters listed in table 1

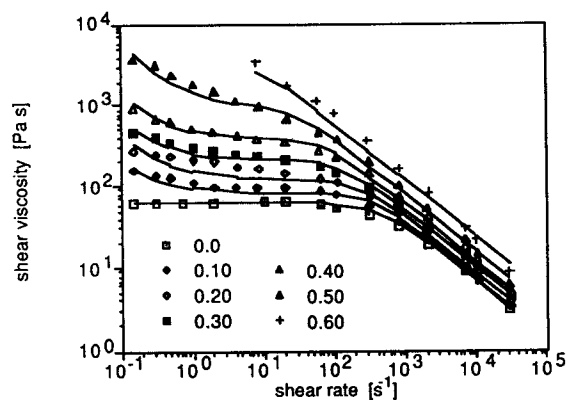


Fig. 7. Steady shear viscosity of Silicone oil filled with coal particles. Data taken from Gleissle and Baloch [24]; solid curve calculated from eq. (11) using the parameters listed in table 2

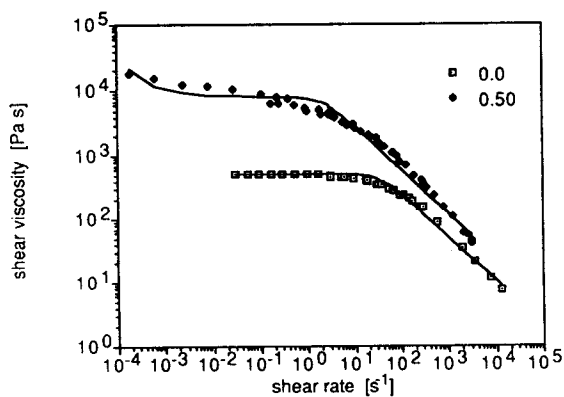


Fig. 8. Steady shear viscosity of Polydimethylsiloxane filled with glass beads. Solid curve calculated from eq. (11) using the parameters listed in table 3

Table 1. Parameters for calculating viscosity curves

|                             | vol.-<br>fraction<br>[%] | $\tau_0$<br>[Pa] | $\eta_0$<br>[Pa s] | $\lambda$<br>[s] | $n$   |
|-----------------------------|--------------------------|------------------|--------------------|------------------|-------|
| Figure 3                    | 0                        | 0                | 240 000            | 157              | 0.470 |
| HDPE-0.1/<br>$\text{TiO}_2$ | 4.2                      | 100              | 271 000*           | 177**            | 0.470 |
|                             | 12.7                     | 250              | 362 000*           | 237**            | 0.470 |
|                             | 21.6                     | 900              | 526 000*           | 344**            | 0.470 |
| Figure 4                    | 0                        | 0                | 5 560              | 2.20             | 0.525 |
| LDPE-5/<br>$\text{TiO}_2$   | 4.3                      | 12               | 6 290*             | 2.49**           | 0.525 |
|                             | 13.0                     | 150              | 8 490*             | 3.36**           | 0.525 |
|                             | 22.1                     | 525              | 12 500*            | 4.94**           | 0.525 |
|                             | 36.0                     | 4 400            | 27 000*            | 10.7**           | 0.525 |
| Figure 5                    | 0                        | 0                | 690                | 0.380            | 0.690 |
| LDPE-23/<br>$\text{TiO}_2$  | 4.3                      | 20               | 780*               | 0.430**          | 0.690 |
|                             | 13.0                     | 225              | 1 050*             | 0.580**          | 0.690 |
|                             | 22.1                     | 2 400            | 1 550*             | 0.853**          | 0.690 |
|                             | 36                       | 17 000           | 3 350*             | 1.84**           | 0.690 |
| Figure 6                    | 0                        | 0                | 16 900             | 2.85             | 0.415 |
| PS/ $\text{TiO}_2$          | 4.8                      | 3.5              | 19 400*            | 3.27**           | 0.415 |
|                             | 14.3                     | 31               | 27 100*            | 4.58**           | 0.415 |
|                             | 24.0                     | 700              | 41 500*            | 7.00**           | 0.415 |
|                             | 38.6                     | 0                | 97 800*            | 16.5**           | 0.415 |

\* calculated from eq. (24), \*\* calculated from eq. (25).

Table 2. Parameters for calculating viscosity curves

|                           | vol.-<br>fraction | $\tau_0$<br>[Pa] | $\eta_0$<br>[Pa s] | $\lambda$<br>[s] | $n$   |
|---------------------------|-------------------|------------------|--------------------|------------------|-------|
| Figure 7                  | 0                 | 0                | 61.3               | 0.0024           | 0.310 |
| Si oil/<br>glass<br>beads | 0.10              | 13               | 83.8*              | 0.00328**        | 0.310 |
|                           | 0.20              | 30               | 125*               | 0.00489**        | 0.310 |
|                           | 0.30              | 50               | 206*               | 0.00807**        | 0.310 |
|                           | 0.40              | 100              | 393*               | 0.0154**         | 0.310 |
|                           | 0.50              | 550              | 947*               | 0.0370**         | 0.310 |
|                           | 0.60              | 0                | 3700*              | 0.145**          | 0.310 |

\* calculated from eq. (24), \*\* calculated from eq. (25)

Table 3. Parameters for calculating viscosity curves

|                         | vol.-<br>fraction | $\tau_0$<br>[Pa] | $\eta_0$<br>[Pa s] | $\lambda$<br>[s] | $n$   |
|-------------------------|-------------------|------------------|--------------------|------------------|-------|
| Figure 8                | 0                 | 0                | 530                | 0.029            | 0.310 |
| PDMS/<br>glass<br>beads | 0.50              | 0                | 8 230*             | 0.448**          | 0.310 |

\* calculated from eq. (24), \*\* calculated from eq. (25)



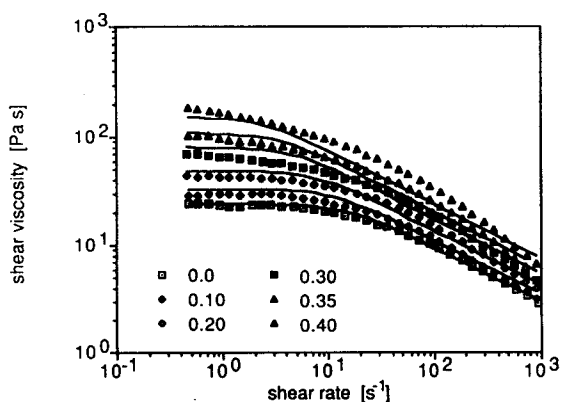


Fig. 9. Steady shear viscosity of Polyisobutylene in decalin filled with glass beads. Data taken from Nicodemo, Nicolais and Landel [30]; solid curve calculated from eq. (11) using the parameters listed in table 4

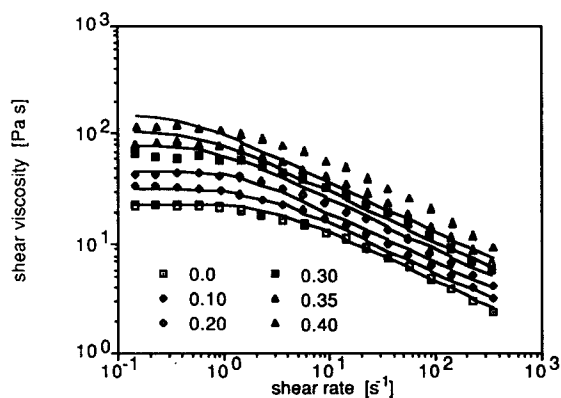


Fig. 10. Steady shear viscosity of aqueous Polyethylene oxide filled with glass beads. Data taken from Nicodemo, Nicolais and Landel [30]; solid curve calculated from eq. (11) using the parameters listed in table 4

Table 4. Parameters for calculating viscosity curves

|                        | vol.-<br>fraction | $\tau_0$<br>[Pa] | $\eta_0$<br>[Pa s] | $\lambda$<br>[s] | $n$   |
|------------------------|-------------------|------------------|--------------------|------------------|-------|
| Figure 9               | 0                 | 0                | 24.1               | 0.0650           | 0.500 |
| PIB/<br>glass<br>beads | 0.10              | 0                | 32.9*              | 0.0889**         | 0.500 |
|                        | 0.20              | 0                | 49.1*              | 0.132**          | 0.500 |
|                        | 0.30              | 0                | 81.1*              | 0.223**          | 0.500 |
|                        | 0.35              | 0                | 109*               | 0.295**          | 0.500 |
|                        | 0.40              | 0                | 154*               | 0.416**          | 0.500 |
| Figure 10              | 0                 | 0                | 23.0               | 0.350            | 0.550 |
| PEO/<br>glass<br>beads | 0.10              | 0                | 31.4*              | 0.478**          | 0.550 |
|                        | 0.20              | 0                | 46.9*              | 0.714**          | 0.550 |
|                        | 0.30              | 0                | 77.4*              | 1.18**           | 0.550 |
|                        | 0.35              | 0                | 104*               | 1.59**           | 0.550 |
|                        | 0.40              | 0                | 148*               | 2.24**           | 0.550 |

\* calculated from eq. (24), \*\* calculated from eq. (25)

viscosity curve for the filled polydimethylsiloxane is slightly different to that of the unfilled fluid, that of the filled fluid being more rounded. This change in shape contradicts the assumptions leading to eq. (21) – which allows the shifting of the viscosity curve with no change in shape. This “rounding” of the viscosity curve may be due to the fact that, in the filled fluid, the deformation rate in the fluid between the particles is not homogeneous and different parts of the fluid are deformed at different rates; this is opposite to the unfilled fluid which is sheared homogeneously. Shifting the time constant  $\lambda$  can account for the increase in the local average deformation rate, but cannot account for the fact that there exists a wide range of deformation rates in the filled fluid.

The proposed equation closely describes the viscosity of filled polymer melts. To test its applicability to filled polymer solutions, predictions of the equation were compared with data of Nicodemo et al. [30] for glass bead filled polymer solutions. Shown in figure 9 is the viscosity of a 0.043 g/cm<sup>3</sup> solution of polyisobutene in decalin filled with glass beads having diameters from 4 to 44  $\mu\text{m}$ . The parameters used are listed in table 4. The viscosity curve for the unfilled solution is somewhat more rounded than that described by eq. (26). The unfilled solution seems to have a broad dispersion of time constants, and a single time constant may not be sufficient to describe the viscosity data. For the filled solution, good agreement is obtained at low shear rates, but at high rates, the viscosity curve is again more rounded than the curve predicted by eq. (26). It appears that the breadth of the time constant dispersion for the solution is amplified by the presence of the filler.

In figure 10, the viscosity of a 0.066 g/cm<sup>3</sup> aqueous solution of polyethylene oxide (PEO) filled with glass beads is shown. The predicted viscosity is too low at high shear rates. The observed viscosity curve does not exhibit the predicted horizontal shift with increasing solid volume fraction. Apparently, approximations made in the model, eq. (26), are not valid for this material. It is tempting to ascribe the discrepancy between the observed and predicted viscosity curves to changes in the viscosity of the suspending PEO solutions with increasing filler concentration. It is known that the viscosity of aqueous solutions of PEO is sensitive to small concentrations of salts [31]. The presence of ions at the surface of the glass beads would have changed the viscosity of the PEO solution. It is also known that PEO solutions undergoing shear are susceptible to mechanical degradation [32]. It could be imagined that with the addition of filler, the local deformation rate in the fluid could be high enough to break PEO molecules and thus decrease the shear thinning of the solution. Nicodemo et al. [30] were very careful in preparing the solution and removed any impu-

rities from the glass beads by washing them with distilled water and acid and extracting them with isopropanol. Also, repeated viscosity measurements were made to rule out changes which would accompany mechanical degradation.

An attempt was made to fit data of Nicodemo et al. [30] for an aqueous solution of sodium carboxymethylcellulose (SCMC) filled with glass beads. It was found that eq. (26) overestimated the viscosity in the plateau region, that is, eq. (24) did not predict the correct solid volume fraction dependence of the parameter  $\eta_0$ . This is surprising and indicates that non-hydrodynamic effects are non-negligible at higher shear rates, making the additivity assumption of eq. (1) incorrect, or indicates that variables other than the solid volume fraction can affect the relative viscosity of a filled polymer solution, or indicates that the viscosity of the polymer solution is changed upon the addition of the glass beads.

It was noted by Nicodemo et al. [30] that the viscosity of aqueous solutions of SCMC is variable with pH and efforts were made to control the pH of the suspensions. It may be possible, despite the careful work of Nicodemo et al., that the pH of the suspensions varied with the concentration of glass beads. This is consistent with the observation that for the filled PEO solutions, which are not as sensitive to pH, correct viscosities were predicted at low shear rates. It is also possible that non-hydrodynamic interactions are non-negligible at high rates for the filled SCMC solutions.

The dependence of the viscosity of some filled polymer solutions is different than that of filled polymer melts. It appears that non-hydrodynamic effects may influence the viscosity of filled polymer solutions even at high rates. This is not taken into account in the additivity assumption of eq. (1). In a polymer melt with a high viscosity, hydrodynamic forces on the particles is large, even at moderate shear rates, and are dominant over non-hydrodynamic forces. In a polymer solution, which has a much lower viscosity than a polymer melt, hydrodynamic forces may not dominate over non-hydrodynamic forces, even at large shear rates. Thus, the additivity assumption may not be applied to such suspensions.

## 5. Conclusion

Filled polymer melts exhibit apparent yielding and shear thinning. Yielding results from non-hydrodynamic particle-particle interactions, while shear thinning results from the non-Newtonian behavior of the polymer melt. A simple equation, based on the linear superposition of the two effects, can accurately describe the viscosity of

filled polymer melts, over a wide range of shear rates and filler volume fraction.

Parameters in the equation are closely related to properties of the unfilled polymer melt and to the solid volume fraction, so that the resulting equation has only one adjustable parameter. The viscosity predicted by the equation was compared with the experimental data for filled polymer melts and filled polymer solutions and a good agreement was obtained. A good agreement was not obtained with the experimental data for aqueous polymer solutions, indicating that non-hydrodynamic interactions may be important at high shear rates for these materials.

The scalar equation proposed describes only the steady shear viscosity. It should be noted that a general constitutive equation can be constructed from the superposition of two relaxation mechanisms. Analogously to eq. (1), the stress tensor may be written:

$$\tau = \tau_I + \tau_{II} \quad (27)$$

Winter et al. [33] have proposed a two-term memory-integral constitutive equation which gives the stress tensor in transient flows. The first term of the memory function describes apparent yielding and the second term describes strain thinning and non-linear viscoelastic behavior. The superposition of two very different relaxation mechanisms qualitatively describes the flow behavior of many fluids with an internal structure. The superposition principle may be generalized to include more than two terms. In the limit of an infinite number of terms the memory function becomes a functional, dependent upon the entire history of the deformation, and the most general form of single memory-integral constitutive equation for a simple fluid is obtained.

## Acknowledgement

The authors wish to thank the Office of Naval Research for financial support (Contract no. N0014-85-K-0880).

## References

1. Metzner AB (1985) *Trans Soc Rheol* 29:739-775
2. Kamal MR, Mutel A (1985) *J Polym Engng* 5:293-382
3. Glushkov IA, Vinogradov GV, Rozhkov VA (1976) *Polym Mech* 10:779-783
4. White, JL (1979) *J Non-Newtonian Fluid Mech* 5:177-190
5. Herschel WH, Bulkley R (1926) *Kolloid-Z* 39:291-300
6. Krieger IM, Dougherty TJ (1959) *Trans Soc Rheol* 3:137-152
7. Barnes HA, Walters K (1985) *Rheol Acta* 24:323-326
8. Matsumoto TC, Hitomi C, Onogi C (1975) *Trans Soc Rheol* 10:541-555
9. Matsumoto TC, Yamamoto O, Onogi S (1980) *Trans Soc Rheol* 24:379-394

10. Tsai SC, Viers B (1987) *J Rheol* 31:483-494
11. Landel RF, Moser BG, Bauman AJ (1963) *Proc IV Intl Congr Rheol* 3:663-692
12. Giesekus H (1978) *ZAMM* 58:T26-T37
13. Michele J, Pätzold R, Donis R (1977) *Rheol Acta* 16:317-321
14. Hoffman RL (1972) *Trans Soc Rheol* 16:155-173
15. Pätzold R (1980) *Rheol Acta* 19:322-344
16. Husband DM, Gadala-Maria F (1987) *J Rheol* 31:95-110
17. Gadala-Maria F, Acrivos A (1980) *Trans Soc Rheol* 24:799-814
18. Gadala-Maria FA (1979) PhD diss, Stanford Univ, Stanford
19. Minagawa N, White JL (1976) *J Appl Polym Sci* 20:501-520
20. Laun HM (1984) *Angew Makromol Chem* 123/124:335-359 (2012)
21. Windhab E, Gleissle W (1984) *Proc. IX Intl. Congr Rheol* 2:557-564
22. Leighton DT, Acrivos A (1986) *Chem Engng Sci* 41:1377-1384
23. Carreau PJ (1968) PhD Thesis, Univ of Wisconsin, Madison
24. Gleissle W, Baloch MK (1984) *Proc. IX Intl. Congr Rheol*, 2:549-556
25. Thomas DG (1965) *J Colloid Sci* 20:267-277
26. Rutgers IR (1962) *Rheol Acta* 2:305-348
27. Graham AL, Steele RD, Bird RB (1984) *Ind Engng Chem Fund* 23:420-425
28. Nicodemo L, Nicolais L (1974) *J Appl Polym Sci* 18:2809-2818
29. Stephens TS (1988) PhD diss, Univ Massachusetts, Amherst
30. Nicodemo L, Nicolais L, Landel RF (1974) *Chem Engng Sci* 29:729-735
31. Bailey FE Jr., Powell GM, Smith KL (1958) *Ind Engng Chem* 50:8-11
32. Clinton N, Matlock, P (1985) *Encyclopedia of Polym Sci and Engng* vol 6:225-273
33. Winter HH, Stephens TS, Morrison FM (1985) 56th annual meeting Soc Rheol, Blacksburg, Virginia (unpublished)

(Received September 14, 1987)

Authors' addresses:

Dr. T. S. Stephens, Prof. H. H. Winter \*)  
Department of Chemical Engineering  
University of Massachusetts  
Amherst, MA 01003 (U.S.A.)

Dr. M. Gottlieb  
Department of Chemical Engineering  
Ben-Gurion University  
Beer Sheva (Israel)

\*) To whom correspondence should be sent